

# A NEXT-TO-LEADING-ORDER QCD ANALYSIS OF NEUTRINO CHARM PRODUCTION: PROBING NUCLEON STRANGENESS

A.O. Bazarko, C.G. Arroyo, K.T. Bachmann, R.E. Blair, T. Bolton,  
C. Foudas, B.J. King, W.C. Lefmann, W.C. Leung, S.R. Mishra, E. Oltman,  
P.Z. Quintas, S.A. Rabinowitz, F.J. Sciulli, W.G. Seligman, M.H. Shaevitz  
*Columbia University, New York, NY 10027*

F.S. Merritt, M.J. Oreglia, B.A. Schumm  
*University of Chicago, Chicago, IL 60637*

R.H. Bernstein, F. Borcharding, H.E. Fisk, M.J. Lamm,  
W. Marsh, K.W.B. Merritt, H.M. Schellman, D.D. Yovanovitch  
*Fermilab, Batavia, IL 60510*

A. Bodek, H.S. Budd, P. de Barbaro, W.K. Sakumoto  
*University of Rochester, Rochester, NY 14627*

T. Kinnel, P.H. Sandler, W.H. Smith  
*University of Wisconsin, Madison, WI 53706*

(CCFR Collaboration)

*Presented by Andrew O. Bazarko at the  
XXVIIIth Rencontre de Moriond: QCD and High Energy Hadronic Interactions,  
20-27 March 1993*

## ABSTRACT

We present the first next-to-leading-order QCD analysis of neutrino charm production. The analysis is based on a study of 5030  $\nu_\mu$ - and 1060  $\bar{\nu}_\mu$ -induced opposite-sign dimuon events, which were gathered from two neutrino-nucleon scattering runs at the Fermilab Tevatron. We measure the charm quark mass,  $m_c = 1.61 \pm 0.26 \text{ GeV}/c^2$ , which may be compared to measurements derived from similar analyses of charm production by other processes. The nucleon strange quark content is found to be suppressed with respect to the non-strange sea quarks by a factor  $\kappa = 0.435 \pm 0.059$  and the strange sea  $x$ -dependence is found to be similar to that of the non-strange sea. The strange sea is needed for the comparison of CCFR structure function measurements with those obtained from charged-lepton scattering. Good agreement is observed between the neutrino and charged lepton measurements for  $x > 0.1$ , but there is a 5 to 10 % discrepancy below that value. Recent global fits by the CTEQ Collaboration that explain this discrepancy by a large strangeness content are shown to be inconsistent with the direct measurement of  $xs(x)$  presented here.



## 1. Introduction

Deep-inelastic neutrino-nucleon scattering offers the unique opportunity to resolve the strange quark content of the nucleon. The strange sea is probed through charm quark production, whose distinct experimental signature is the presence of opposite sign dimuons in the final state. One muon is associated with the incoming  $\nu_\mu$  or  $\bar{\nu}_\mu$ , and the other with the decay of the  $c$  or  $\bar{c}$ .

$$\nu_\mu + \left( \begin{smallmatrix} s \\ d \end{smallmatrix} \right) \longrightarrow \mu^- + c \hookrightarrow s \mu^+ \nu_\mu$$

The corresponding  $\bar{\nu}_\mu$  process has the  $s$ ,  $d$ , and  $c$  quarks replaced by their antiquark partners and oppositely charged muons.

We present the first next-to-leading-order (NLO) QCD analysis of neutrino charm production. The preliminary results reported here are from data taken in two runs at the Fermilab Tevatron Quad-Triplet beam, E744 and E770, with neutrino energies up to 600 GeV. A sample of 3.7 million triggers yielded 15000 multi-muon candidate events, which were further reduced after fiducial and kinematic cuts ( $P_{\mu_1} \geq 9$  GeV/c,  $P_{\mu_2} \geq 5$  GeV/c,  $E_{HAD} > 10$  GeV,  $\theta_\mu < 0.250$ ,  $Q_{vis}^2 > 1$  GeV<sup>2</sup>/c<sup>2</sup>) to 5030  $\nu_\mu$ - and 1060  $\bar{\nu}_\mu$ -induced  $\mu^\mp \mu^\pm$  events. Results from a leading-order analysis of this data sample were reported previously.<sup>1</sup>

## 2. The Next-to-Leading-Order Cross Section

The heavy charm quark introduces an energy threshold in the dimuon production rate. This effect relates  $\xi$ , the momentum fraction of the struck quark, to the kinematic variable  $x = Q^2/2ME_\nu y$ , through the expression

$$\xi = x \left( 1 + \frac{m_c^2}{Q^2} \right) \left( 1 - \frac{x^2 M^2}{Q^2} \right)$$

where  $Q^2$  is the negative square of the four-momentum transfer,  $y$  is the inelasticity and  $M$  is the nucleon mass. Kinematic corrections for a massive initial state strange quark are also included in the results presented.

The differential cross section for dimuon production is expressed generally as

$$\frac{d^3\sigma(\nu_\mu N \rightarrow \mu^- \mu^+ X)}{d\xi dy dz} = \frac{d^2\sigma(\nu_\mu N \rightarrow cX)}{d\xi dy} D(z) B_c(c \rightarrow \mu X)$$

where the function  $D(z)$  describes the hadronization of charmed quarks and  $B_c$  is the semi-muonic branching ratio of the charmed hadrons. The leading-order charm production differential cross section for an isoscalar target is given by:

$$\left\{ \frac{d^2\sigma(\nu_\mu N \rightarrow cX)}{d\xi dy} \right\}_{LO} = \frac{G^2 M E_\nu}{\pi} \left( [\xi u(\xi) + \xi d(\xi)] |V_{cd}|^2 + \xi s(\xi) |V_{cs}|^2 \right) \left( 1 - \frac{m_c^2}{2ME_\nu \xi} \right)$$

where  $\xi u(\xi)$ ,  $\xi d(\xi)$  and  $\xi s(\xi)$  represent the momentum distributions of the  $u$ ,  $d$  and  $s$  quarks within the nucleon, and Callan-Gross violation has been neglected for brevity.

Recent theoretical work has extended the leading-order formalism of neutrino charm production to next-to-leading-order. Because a dominant contribution to this process is scattering off strange quarks, the NLO gluon-initiated contributions are significant. The NLO charm production differential cross section calculation of Aivazis, Olness and Tung<sup>2</sup> used here includes the Born and gluon-fusion diagrams, shown in Figure 1. The calculation was performed in the  $\overline{MS}$  scheme and the renormalization scale was chosen to be  $\mu = 2p_\perp^{\max}$ , where  $p_\perp^{\max}$  is the maximum available transverse momentum of the initial state quark coming from the gluon splitting, or equivalently of the final state charm quark, for the given kinematic variables  $x$  and  $Q^2$ .

### 3. Fit Results

Information about the strange sea, the branching ratio, and the charm mass parameter is extracted by comparing the  $x_{vis}$  and  $E_{vis}$  distributions of the data to a Monte Carlo simulation. The Monte Carlo simulates both single muon and dimuon events, in order to model the detector acceptance, resolution smearing, and missing energy associated with the charm decay.

The gluon and singlet ( $q + \bar{q}$ ) and nonsinglet ( $q - \bar{q}$ ) quark distributions are obtained from next-to-leading-order QCD fits<sup>3</sup> to the CCFR structure functions<sup>4</sup> using the evolution programs of Duke and Owens.<sup>5</sup> To resolve the strange component of the quark sea, the strange quark  $x$  dependence is assumed to be related to the  $\bar{q}$  distribution by  $xs(x) \propto (1-x)^\alpha x \bar{q}(x)$ . The strange quark magnitude is set by the parameter  $\kappa = 2S/(\bar{U} + \bar{D})$ , where  $S = \int_0^1 xs(x) dx$ , etc. The overall normalization is set by the ratio of data to Monte Carlo for the charged-current single muon events. Because the neutrino target is nearly isoscalar, the analysis is insensitive to the exact form of the up and down quark distributions.

The largest source of systematic uncertainty is charm quark hadronization, which is parameterized by the Peterson fragmentation function,  $D(z) \propto \{z[1 - (1/z) - \epsilon/(1-z)]^2\}^{-1}$ , where  $z = P_D/P_c$  is the ratio of the charmed meson and quark momenta.<sup>6</sup> The Monte Carlo is fit to the data for various fixed values of the adjustable Peterson parameter  $\epsilon$ , and a study of the distribution of  $z_{vis} = E_{\mu_2}/(E_{\mu_2} + E_{had})$  combined with an analysis of E531 neutrino emulsion data<sup>7</sup> yields a neutrino average  $\epsilon = 0.20 \pm 0.04$ .

The dimuon events are divided into those from incident  $\nu_\mu$  or  $\bar{\nu}_\mu$  by assuming that the leading muon has larger transverse momentum with respect to the direction of the hadron shower than the muon from charm decay. Monte Carlo studies indicate that this identification procedure introduces a  $1.1 \pm 0.2\%$  ( $32 \pm 2\%$ ) contamination in the  $\nu_\mu$  ( $\bar{\nu}_\mu$ ) sample. Muonic decays of non-prompt  $\pi$  and  $K$  mesons in the hadron shower of the charged-current events constitute the primary source of dimuon background. Hadronic test beam muoproduction data and Monte Carlo simulations predict a  $\pi/K$  decay background of  $797 \pm 118 \nu_\mu$  and  $118 \pm 25 \bar{\nu}_\mu$  events.<sup>8</sup>

The extracted parameters with their statistical and systematic errors are presented in the following Table along with the previous leading-order results.<sup>1</sup> The fits contain 46 degrees of freedom.

	$\chi^2$	$\kappa$	$\alpha$	$B_c$	$m_c$
NLO fit	41.3	0.435 $\pm 0.055 \pm 0.020$	-0.27 $\pm 0.60 \pm 0.40$	0.102 $\pm 0.007 \pm 0.005$	1.61 $\pm 0.22 \pm 0.13$
LO fit	42.5	0.373 $^{+0.048}_{-0.041} \pm 0.018$	2.50 $^{+0.60}_{-0.55} \pm 0.36 \pm 0.25$	0.105 $\pm 0.007 \pm 0.005$	1.31 $^{+0.20}_{-0.22} \pm 0.12 \pm 0.11$

### 4. Comparisons and Conclusions

The charm quark mass parameter from the NLO fit is  $1.61 \pm 0.26 \text{ GeV}/c^2$ , which differs from our leading-order result, indicating the marked dependence of this quantity on the order to which the analysis is done. This value of  $m_c$  may be compared to measurements derived from other processes involving similar perturbative QCD calculations. A photon-gluon-fusion analysis of photoproduction data<sup>9</sup> finds  $m_c = 1.74^{+0.13}_{-0.18}$ .

The nucleon strangeness content is found to be  $\kappa = 2S/(\bar{U} + \bar{D}) = 0.435 \pm 0.059$ , indicating that the sea is not SU(3) symmetric, which is consistent with previous LO analyses. The  $x$ -dependence of the strange sea is found to be similar to that of the non-strange sea, with the shape parameter  $\alpha = -0.27 \pm 0.72$ . This differs from LO analyses, which find that to leading-order the strange sea is softer than its non-strange counterparts.

The strange sea can also be inferred from a comparison of charged lepton and neutrino structure functions. To leading-order the lepton and neutrino structure functions are related by the "5/18ths rule":

$$\frac{F_2^{lN}}{F_2^{\nu N}} = \frac{5}{18} \left( 1 - \frac{3s + \bar{s}}{5q + \bar{q}} \right)$$

where the strange sea enters as a correction. Our CCFR results span the  $Q^2$  range from the low energy SLAC<sup>10</sup> (eD) region through the range covered by the NMC<sup>11</sup> and BCDMS<sup>12</sup> ( $\mu$ D) measurements. For this comparison, the deuterium data are corrected to iron using the  $F_2^{Fe}/F_2^D$  ratio measured by SLAC<sup>13</sup> and NMC.<sup>11</sup> The comparison shows good agreement for  $x > 0.1$  but a 5 to 10% discrepancy is seen between the neutrino and muon results for lower  $x$ . The source of this small disagreement is at present not known. Possible sources include experimental systematic errors related to normalization and calibration or theoretical uncertainties associated with the heavy target correction, the value of  $R(x, Q^2) \equiv \sigma_L/\sigma_T$  for neutrinos, and higher-order effects. Recent global fits by Botts *et al.* of the CTEQ collaboration have attributed the muon versus neutrino difference to an enhanced strange sea at low  $x$ .<sup>14</sup> This possibility is ruled out by our dimuon measurements, as shown in Figure 2.

This research was funded by the United States Department of Energy and the National Science Foundation.

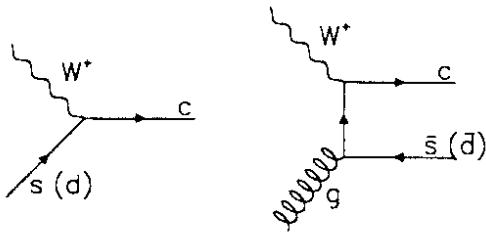


Figure 1: Mechanisms that contribute to neutrino production of charm.

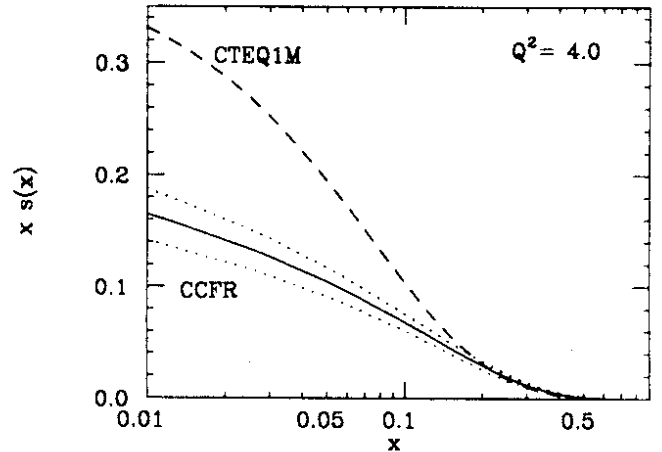


Figure 2: The strange quark distribution function extracted from the CCFR dimuon data compared to the distribution of the CTEQ global fit. The band on the CCFR curve indicates the  $1\sigma$  uncertainty in the distribution.

## References

1. S.A. Rabinowitz *et al.*, *Phys. Rev. Lett.* **70** (1993) 134.
2. M.A.G. Aivazis, F.I. Olness, and W.K. Tung, *Phys. Rev. Lett.* **65** (1990) 2339.
3. W.G. Seligman *et al.*, these proceedings.
4. S.R. Mishra *et al.*, Nevis-1459 (1992), submitted to *Phys. Lett.*; W.C. Leung *et al.*, Nevis-1460 (1992), submitted to *Phys. Lett.*; P.Z. Quintas *et al.*, Nevis-1461 (1992), submitted to *Phys. Rev. Lett.*
5. D. Duke and J. Owens, *Phys. Rev.* **D30** (1984) 49.
6. C. Peterson *et al.*, *Phys. Rev.* **D27** (1983) 105.
7. N. Ushida *et al.*, *Phys. Lett.* **B121** (1983) 292.
8. P.H. Sandler *et al.*, *Z. Phys.* **C57** (1993) 1.
9. J.C. Anjos *et al.*, *Phys. Rev. Lett.* **65** (1990) 2503.
10. L. Whitlow, Ph.D. Thesis, Stanford University, SLAC-Report-357 (1990).
11. P. Amaudruz *et al.*, *Phys. Lett.* **B295** (1992) 159.
12. A.C. Benvenuti *et al.*, *Phys. Lett.* **B223** (1989) 485; **B237** (1990) 592.
13. A. Bodek *et al.*, *Phys. Rev. Lett.* **50** (1983) 1431; **51** (1983) 534.
14. J. Botts *et al.*, *Phys. Lett.* **B304** (1993) 159.